Fungal Genetics and Biology 46 (2009) 642–656

Contents lists available at ScienceDirect

Fungal Genetics and Biology

journal homepage: www.elsevier.com/locate/yfgbi

A polyphasic approach to the taxonomy of the *Alternaria infectoria* species–group

Birgitte Andersen [a,*], Jens Laurids Sørensen [a], Kristian Fog Nielsen [a], Bert Gerrits van den Ende [b], Sybren de Hoog [b]

[a] Center for Microbial Biotechnology (CMB), Department of Systems Biology, Building 221, Technical University of Denmark, DK-2800 Kgs. Lyngby, Denmark
[b] Centraalbureau voor Schimmelcultures (CBS-KNAW), Fungal Biodiversity Centre, P.O. Box 85167, 3508 AD Utrecht, The Netherlands

ARTICLE INFO

Article history:
Received 20 December 2008
Accepted 28 May 2009
Available online 6 June 2009

Keywords:
Chemical classification
Fungi
Haplotypes
Molecular cladification
Morphology
Multivariate statistics
Recombinants

ABSTRACT

Different taxa in the species–group of *Alternaria infectoria* (teleomorph *Lewia* spp.) are often isolated from various cereals including barley, maize and wheat grain, ornamental plants and skin lesions from animals and humans. In the present study we made a polyphasic characterization of 39 strains morphologically identifiable as belonging to the *A. infectoria* species–group together with 12 strains belonging to closely related species: *Alternaria malorum* (syn. *Cladosporium malorum*), *Chalastospora cetera* (syn. *Alternaria cetera*) and *Embellisia abundans*. Morphological examination separated the 51 strains in three groups based on conidial appearance and arrangement: the *A. infectoria* species–group, *E. abundans* and a group containing *C. cetera* and *A. malorum*. The metabolite analyses on three different media showed two clusters, one containing all 39 *A. infectoria* species–group strains and one containing 10 strains of *E. abundans*, *C. cetera* and *A. malorum*. One *E. abundans* strain and one *A. malorum* strain were not included due to insufficient metabolite production. The separation of the *A. infectoria* species–group from *E. abundans*, *C. cetera* and *A. malorum* resulted mainly from the ability to produce altertoxins and novae-zelandins. The metabolite analyses also showed that all 51 strains were able to produce infectopyrones. The metabolite profiles of *C. cetera* and *A. malorum* were very similar with several metabolites of unknown structure in common. This is the first time that *E. abundans*, *C. cetera* and *A. malorum* have been reported as producers of infectopyrones. Sequence analyses of the internal transcribed spacer region (ITS), glyceraldehyde-3-phosphate dehydrogenase (*gpd*) and translocation elongation factor 1α (*tef-1α*) showed two clades: one with the 39 strains from the *A. infectoria* species–group and one with the 12 strains of *E. abundans*, *C. cetera* and *A. malorum*. The polyphasic approach in this study suggests that *A. malorum* var. *polymorpha* and the eight *A. malorum* strains do not belong in *Alternaria*, but in *Chalastospora*, however, as several distinct species. Splits Tree alignment of *gpd* sequences of 38 strains belonging to the *A. infectoria* species–group indicates that only three strains showed signs of recombination, while the remaining strains appeared to be clonal. Long term incubation at 7 °C in the dark showed that 12 out of 33 tested strains from the *A. infectoria* species–group were able to produce proascomata in axenic culture, but with no mature ascospores after 6 months. These findings suggest that *Lewia*/*A. infectoria* species–group must, at least in part, be homothallic. The results presented in this study show that ITS, *tef-1α* and *gpd* do not reflect ecology, secondary metabolism or morphology of the *A. infectoria* species–group and that molecular cladification and phylogeny cannot predict pathogenicity, host specificity or mycotoxin production.

1. Introduction

The *Alternaria infectoria* EG Simmons species–group *sensu* Simmons (Simmons and Roberts, 1993; Simmons, 2007) comprises more than 30 named anamorph taxa, among which *Alternaria arbusti* EG Simmons, *Alternaria ethzedia* EG Simmons, *A. infectoria*, *Alternaria intercepta* EG Simmons, *Alternaria metachromatica* EG Simmons, *Alternaria oregonensis* EG Simmons, *Alternaria photistica* EG Simmons, *Alternaria triticimaculans* EG Simmons, *Alternaria triticina*, *Alternaria viburni* EG Simmons are some (Simmons, 2007). It is the only group in *Alternaria* where some members have a teleomorph state, *Lewia* ME Barr and EG Simmons (Simmons, 1986). Morphologically, the *A. infectoria* species–group differs from other *Alternaria* species–groups in the three-dimensional sporulation pattern (Simmons and Roberts, 1993). Characteristic for the *A. infectoria* species–group is the production of small conidia (up to 70 μm in length) in branched chains with long, geniculate multilocus secondary conidiophores (up to 120 μm) between conidia (Simmons, 2007).

Chemically, the *A. infectoria* species–group is very different from other *Alternaria* species, producing metabolites that are not found

* Corresponding author. Fax: +45 4588 4922.
E-mail address: ba@bio.dtu.dk (B. Andersen).

1087-1845/$ - see front matter © 2009 Elsevier Inc. All rights reserved.
doi:10.1016/j.fgb.2009.05.005

in other species–groups (Andersen and Thrane, 1996). None of the taxa in the *A. infectoria* species–group has ever been shown to produce alternariols or tenuazonic acid, which are common in other small-spored *Alternaria* species (Andersen et al., 2002) or altersolanols, common in some large-spored *Alternaria* (Andersen et al., 2008). On the other hand, taxa in the *A. infectoria* species–group produce infectopyrones and novae-zelandins (Christensen et al., 2005), which have never been detected in other *Alternaria* species–groups. However, infectopyrones have been found in other genera, such as *Phoma* Sacc., *Stemphylium* Wallr. and *Ulocladium* Preuss (Pedras and Chumala, 2005; Christensen et al., 2005; Andersen and Hollensted, 2008, respectively).

Molecularly, taxa in the *A. infectoria* species–group have been analyzed at the sub-genus level using the ribosomal internal transcribed spacer region (ITS), glyceraldehyde-3-phosphate dehydrogenase (*gpd*) and translocation elongation factor 1α (*tef-1α*) sequences and the results showed that the *A. infectoria* species–group constitutes a quite distinct clade (de Hoog and Horré, 2002; Pryor and Bigelow, 2003). Another ITS sequence analysis creating an unrooted radial tree based on maximum likelihood calculation showed that *Alternaria malorum* (Ruehle) U. Braun, Crous and Dugan (*Cladosporium malorum* Ruehle), and the *A. infectoria* species–group comprised a single clade (Braun et al., 2003). An inquiry on *Alternaria* in the CBS database of ITS sequences showed that a strain of *Chalastospora cetera* (EG Simmons) EG Simmons (*Alternaria cetera* EG Simmons) and three strains of *Embellisia abundans* EG Simmons also clustered in the same clade as *A. malorum* and the *A. infectoria* species–group (unpublished results).

Many taxa in the *A. infectoria* species–group are associated with various species in the grass family (*Poaceae* L.). They have been reported from stems, straw, leaves and grains of oat, barley, wheat and rye (Simmons, 1986; Andersen et al., 2002; Dugan and Peever, 2002; Perelló et al., 2008) and are also known to occur on maize (unpublished results). *A. triticina* Prasada and Prabhu, a known plant pathogenic species in the *A. infectoria* species–group, was first reported on wheat in India (Prasada and Prabhu, 1962) and later on the same host plant in Argentina (Perelló and Sisterna, 2006) and in Iran (Simmons, 2007). Other species isolated from discrete lesions of non-poaceae host plants, such as *A. viburni* and *A. ethzedia*, are presumed to have various degrees of pathogenicity (Simmons, personal commun.). In the last decade, taxa in the *A. infectoria* species–group have increasingly been isolated from human cutaneous infections, especially from immuno-compromised patients (de Hoog and Horré, 2002; Dubois et al., 2005; unpublished results).

The objective of this work was to prove the hypothesis that taxa in *Lewia*/*A. infectoria* species–group are sexual fungi and that molecular sequence analysis and metabolite profiling will yield a number of clades and clusters that will correspond to the number of morphological species in the group. Previous research on other genera has shown that sequence analyses reveal cryptic molecular species (Taylor et al., 2000; O'Donnell et al., 2004). Studies on *Penicillium* and large-spored *Alternaria* have shown that results from metabolite profiling correlates with the morphological species concept (Andersen et al., 2008; Frisvad and Samson, 2004). Other research on *Aspergillus* and *Stachybotrys* has shown that molecular sequence analyses correlated with the morphological species concept and metabolite profiling (Samson et al., 2007; Andersen et al., 2003). Furthermore, controversy over whether the *A. infectoria* species–group comprises many species based on morphological differences or consists of only one species based on molecular sequence analysis has arisen. Therefore, this polyphasic study of the *A. infectoria* species–group, including molecular sequence analysis, metabolite profiling and mating tests, was set up. The study also included *A. malorum,* since this species had been reported to belong to the *A. infectoria* species–group (Braun et al., 2003), together with *C. cetera* and *E. abundans*. One aim was to compare chemical and molecular findings with the current morphological classification and examine which factors correlate and which could resolve and segregate *Alternaria* from *Chalastospora* and *Embellisia*. Another aim was to test if other isolates than the human opportunists were able to grow at 37 °C.

2. Materials and methods

2.1. Fungal strains

Fifty-one fungal strains belonging to the *A. infectoria* species–group (39), *A. malorum* (9), *C. cetera* (1), and *E. abundans* (2) were used. Identity, species–group affiliation, identification number, host plant, and geographic origin of all strains are given in Table 1. Strains are available from CBS collection, Fungal Biodiversity Centre, The Netherlands, and IBT collection, Department of Systems Biology, DTU, Denmark.

2.2. Morphological examination

For morphological examination and DNA analysis, each strain was inoculated in three points onto a PCA plate (potato carrot agar; Simmons, 2007) and incubated under standardized conditions (Andersen et al., 2005). In brief: after inoculation the unsealed plates were incubated in one layer for 7 days at 23 °C under an alternating light/dark cycle consisting of 8 h of cool-white fluorescent daylight (tubes: TLD, 36 W/95, Philips, Denmark) and 16 h darkness. Slides for microscopy were made after 7 days using transparent tape preparations (Butler and Mann, 1959) mounted in lactophenol. All unidentified strains were compared with type cultures and descriptions according to Simmons (2007).

For ascoma production under laboratory conditions, strains were transferred to another PCA plate that had been equipped with autoclaved wooden toothpicks to encourage the production of ascomata. In the first trial, each plate was divided into three sectors with three toothpicks. Three different strains were inoculated on the same plate, one in each sector. In the second trial, each plate was divided into two sectors with one toothpick. The same strain was inoculated in both sectors on the same plate. The plates were first incubated as ordinary PCA plates under alternating light at 23 °C for 2 weeks. Then the plates were sealed with para film™, placed up-side-down, and incubated at 7 °C in the dark for 6 months.

For the ability to grow at high temperature, strains were transferred (three points) to PDA plates (potato dextrose agar; Difco, 213400). Plates were allowed to stand at room temperature for one day to ensure that all strains were viable and growing. The edge of the colonies was marked before incubation. After 12 days at 37 °C the colony edges were marked again and the plates were allowed to stand for two days at room temperature. Strains that had resumed their original growth characteristics were recorded as positive.

2.3. Metabolite extraction

For metabolite analyses, each strain was transferred (three points) onto a DRYES plate (dichloran Rose Bengal yeast extract sucrose agar; Frisvad, 1983), a DG18 plate (dichloran 18% glycerol agar [31.5 g/l dichloran glycerol agar base (OXOID, CM0729); 220 ml/l anhydrous glycerol (JT Baker, 7044); 10 mg/l $ZnSO_4 \cdot 7H_2O$ (Merck, 8883); 5 mg/l $CuSO_4 \cdot 5H_2O$ (Riedel-de Haën, 12849); 50 mg/l chloramphenicol (Sigma, C-0378); 50 mg/l chlortetracycline hydrochloride (Sigma, C-4881)]), and a PDA + DN plate (potato dextrose agar [39.0 g/l potato dextrose agar (Difco, 213400),

Table 1
Host, origin and species–group affiliation of the *Alternaria*, *Chalastospora* and *Embellisia* strains and type cultures (T) used in this study.

#[a]	Genus species	species–group[b]	Host	Origin	CBS #	BA #	EGS #
1	*A. infectoria* sp.–grp	inf. sp.–grp.	*Hordeum*, grain	DK, Jutland	120147	704	
2	*A. triticina* T	inf. sp.–grp.	*Triticum*	India	763.84	1207	17–061
3	*A. infectoria* T	inf. sp.–grp.	*Triticum*	UK	112250	1209	27–193
4	*A. oregonensis* T	inf. sp.–grp.	*Triticum*	USA, OR	542.94	1210	29–194
5	*A. photistica* T	inf. sp.–grp.	*Digitalis*	UK	212.86	1211	35–172
6	*A. ethzedia* T	inf. sp.–grp.	*Brassica*	Switzerland	197.86	1215	37–143
7	*A. metachromatica* T	inf. sp.–grp.	*Triticum*	Australia	553.94	1218	38–132
8	*A. triticimaculans* T	inf. sp.–grp.	*Triticum*	Argentina	578.94	1221	41–050
9	*A. infectoria* sp.–grp.	inf. sp.–grp.	*Hordeum*	Italy		1228	42–086
10	*A. infectoria* sp.–grp.	inf. sp.–grp.	*Hordeum*	NZ		1234	43–070
11	*A. infectoria* sp.–grp.	inf. sp.–grp.	*Hordeum*	NZ		1239	43–160
12	*A. intercepta* T	inf. sp.–grp.	*Viburnum*	Europe	119406	1258	49–137
13	*A. viburni* T	inf. sp.–grp.	*Viburnum*	Europe	119407	1259	49–147
14	*A. arbusti* T	inf. sp.–grp.	*Pyrus*	USA, CA	596.93	1263	91–136
15	*A. infectoria* sp.–grp.	inf. sp.–grp.	*Triticum*, grain	DK	120148	1286	
16	*A. infectoria* sp.–grp.	inf. sp.–grp.	*Triticum*, grain	DK	120149	1287	
17	*A. infectoria* sp.–grp.	inf. sp.–grp.	*Hordeum*, grain	DK	120150	1294	
18	*A. infectoria* sp.–grp.	inf. sp.–grp.	*Hordeum*, grain	DK	120151	1312	
19	*A. infectoria* sp.–grp.	inf. sp.–grp.	*Hordeum*, grain	DK	120152	1315	
20	*C. cetera* T		*Elymus*	Australia	110898	1746	41–072
21	*A. malorum*		Soil	Syria	173.80	1747	
22	*A. malorum*		–	USA	148.66	1748	
23	*A. malorum*		–	NZ	114810	1749	
24	*A. malorum*		–	NZ	114809	1750	
25	*A. malorum*		Soil	Lebanon	900.87	1751	
26	*A. malorum* var. *polymorpha*		*Vitis*	USA, WA	112048	1752	
27	*A. malorum*		*Triticum*, straw	SA, Cape Prov.	266.75	1753	
28	*A. malorum*		*Triticum*, grain	USA, OR	216.65	1754	
29	*A. malorum*		*Gossypium*, seed	Turkey	540.75	1755	
30	*E. abundans*		*Dianthus*, seed	UK	535.83	1757	34–063
31	*E. abundans* T		*Fragaria*	NZ	534.83	1758	29–159
32	*A. infectoria* sp.–grp.	inf. sp.–grp.	–	UK	160.79	1759	
33	*A. infectoria* sp.–grp.	inf. sp.–grp.	*Zea*, fresh silage	DK, Jutland		1760	
34	*A. infectoria* sp.–grp.	inf. sp.–grp.	*Zea*, fresh silage	DK, Jutland		1761	
35	*A. infectoria* sp.–grp.	inf. sp.–grp.	*Zea*, fresh silage	DK, N Jutland		1762	
36	*A. infectoria* sp.–grp.	inf. sp.–grp.	*Zea*, fresh silage	DK, N Jutland		1763	
37	*A. infectoria* sp.–grp.	inf. sp.–grp.	*Zea*, fresh silage	DK, NW Jutland		1764	
38	*A. infectoria* sp.–grp.	inf. sp.–grp.	*Zea*, fresh silage	DK, Jutland		1765	
39	*A. infectoria* sp.–grp.	inf. sp.–grp.	*Zea*, fresh silage	DK, S Jutland		1766	
40	*A. infectoria* sp.–grp.	inf. sp.–grp.	*Zea*, fresh silage	DK, Jutland		JLS08	
41	*A. infectoria* sp.–grp.	inf. sp.–grp.	*Zea*, fresh silage	DK, Jutland		JLS09	
43	*A. infectoria* sp.–grp.	inf. sp.–grp.	*Zea*, fresh silage	DK, N Jutland		JLS32	
44	*A. infectoria* sp.–grp.	inf. sp.–grp.	*Zea*, fresh silage	DK, E Jutland		JLS33	
45	*A. infectoria* sp.–grp.	inf. sp.–grp.	*Homo*, skin lesion	Germany	102692		
46	*A. infectoria* sp.–grp.	inf. sp.–grp.	*Hordeum*	UK	116001		
47	*A. infectoria* sp.–grp.	inf. sp.–grp.	*Paeonia*	NL	106.52		
48	*A. infectoria* sp.–grp.	inf. sp.–grp.	*Avena*, straw	–	308.53		
49	*A. infectoria* sp.–grp.	inf. sp.–grp.	*Homo*, skin lesion	Italy	109785		
50	*A. infectoria* sp.–grp.	inf. sp.–grp.	*Homo*, skin lesion	NL	110803		
51	*A. infectoria* sp.–grp.	inf. sp.–grp.	*Homo*, skin lesion	Austria	110804		
52	*A. infectoria* sp.–grp.	inf. sp.–grp.	*Zea*, fresh silage	DK, N Jutland		JLS38	

[a] Analysis number in this study. #42 is not included.
[b] Member of the *A. infectoria* species–group based on morphology.

10 mg/l $ZnSO_4 \cdot 7H_2O$ (Merck, 8883) and 5 mg/l $CuSO_4 \cdot 5H_2O$ (Riedel-de Haën, 12849)] with additional 30 g/l dextrose (BHD, 10117) and additional 3 g/l $NaNO_3$ (Merck, A855537 811). After inoculation, the DRYES, DG18, PDA + DN plates were packed in perforated plastic bags and incubated in darkness at 25 °C prior to extraction.

Metabolites were extracted separately from 14-day-old DRYES, DG18 and PDA + DN cultures. The extractions were done using a micro-scale extraction method modified for *Alternaria* metabolites (Andersen et al., 2005). In brief: three 6-mm agar plugs were cut from the center of the three colonies and the nine plugs were placed in a 2-ml vial. Plugs were extracted with 1.0 ml ethyl acetate containing 1% formic acid (v/v) and ultrasonicated for 60 min. Extracts were transferred to clean 2-ml vials, evaporated to dryness, re-dissolved ultrasonically in 400 μl methanol, and filtered through 0.45-μm PFTE filters (National Scientific Company, Rockwood, TN, USA) into clean 2-ml vials prior to HPLC analysis. Experiments were repeated once on DRYES a year after with all strains and for strains with low metabolite production a third time on DRYES a month later using 18 plugs.

2.4. HPLC-UV–VIS analyses

Metabolite profiling was performed on an Agilent 1100 HPLC system (Agilent, Waldbronn, Germany) equipped a diode array detector collecting two ultraviolet–visible (UV–VIS) spectra per sec from 200 to 600 nm. Samples of 3.0 μl were separations on a 2 × 100 mm Luna 3 μm C18(2) (Phenomenex, Torrance, CA, USA) at 40 °C using a linear water–acetonitrile gradient and a flow of 0.4 ml/min. The gradient started at 15% acetonitrile, reached 100% in 20 min and was held for 5 min. Both eluents contained 50 ppm trifluoro acetic acid. A homologous series of alkylphenones

was analyzed as external retention time references and used to calculate a bracketed retention index (RI) for each detected peak (Frisvad and Thrane, 1987). In this way each metabolite could be identified by its RI value and its UV–VIS spectrum and be recognized in other extracts.

2.5. HPLC-TOF-MS analyses

Metabolite identification was done on the DRYES extracts using on a similar HPLC-DAD system as described above with minor changes: the column was 50 mm long, flow was 0.3 ml/min, and the eluents were buffered with 20 mM formic acid (Nielsen et al., 2005). High resolution MS detection was done on a Time Of Flight mass spectrometer (Water-Micromass, Manchester, UK) scanning m/z 60–900 and m/z 100–2000 in two separate scan functions at different skimmer settings (Nielsen et al., 2005). All samples were analyzed in both positive (ESI^+) and negative electrospray (ESI^-). Extracts were also analyzed using a gradient system optimized for *A. infectoria* metabolites, using a 2 mm × 100 mm 3 μm Gemini Phenyl column (Phenomenex, Torrance, CA, USA) and a gradient starting at 10% acetonitrile, reaching 47% in 17 min and then 100% in 3 min and was held for 4 min. All samples were analyzed in ESI^+ and ESI^-. Metabolite standards (Nielsen and Smedsgaard, 2003) of 4*Z*-infectopyrone, AAL-toxins TA and TB, AK toxin I, altenuene, altenusin, alternariol, alternariol monomethylether, altersolanol A, altertoxin I, macrosporin, maculosin, tentoxin and tenuazonic acid were co-analyzed for verification.

2.6. Data treatment of metabolite profiles

Metabolite profile data from HPLC-UV–VIS were first treated with the Chemical Image Analysis (CIA) program using an algorithm described by Hansen (2003) as stated by Andersen et al. (2008). In brief: the raw HPLC data files, which are quantitative 2-D matrices (x-axis: time, y-axis: wave length, value in matrix: UV–VIS absorbance), were transferred from the HPLC to a standard PC and analyzed by an in-house written chemical image analysis (CIA) program (Hansen, 2003). No manipulations or peak selections were made before processing. Each HPLC file was processed first by a $\log_{10}$ scaling (to account for concentration differences among extracts), then a baseline correction and finally an alignment (to account for drift in baseline and retention time among identical metabolites in different runs) (Hansen, 2003). Each HPLC file was then compared to the other 50 HPLC files, pair-wise, using an algorithm described by Hansen (2003) giving a similarity value for each pair, which was entered into a new matrix. The resulting 51 × 51 similarity matrix was then used to calculate a dendrogram using WARD clustering method.

Based on the result of the CIA, a binary matrix was made manually by scoring each metabolite from four printed HPLC chromatograms as present or absent (137 metabolites for the 51 fungal strains) and subjected to multivariate statistics using Unscrambler version 9.2 (CAMO ASA, Oslo, Norway). The matrix was analyzed using Partial Least Squares Regression (PLS-R) and Principal Component Analysis (PCA). A reduced matrix (124 metabolites and 49 strains) was subjected to cluster analysis using NTSYS-pc version 2.11 N (Exeter Software, Setauket, NY, USA) without standardization using Yule as correlation coefficient and Unweighted Pair-Group Method using arithmetic Averages (UPGMA) as clustering method. The matrix was also analyzed by simple matching and Jaccard similarity coefficients in NTSYS.

For metabolite identification and peak comparison, 12–20 of the largest peaks in the data files from HPLC-TOF-MS were inspected in UV–VIS, ESI^+, ESI^- modes were compared to peaks registered in the Quanlynx 4.1 software (Water-Micromass) using a $\pm m/z$ 0.02 and a retention time limit of ±0.3 min. If possible, a qualifier ion was used for confirmation. Peaks of the metabolite standards mentioned above were also inserted along with predicted ions calculated from the masses of known *Alternaria* metabolites. In the latter case a ±3 min window was used, with the retention time predicted using the log *D* of the compound (calculated using ACD v.10, Advanced Chemical development Inc., Toronto, Canada), which was correlated to retention time of 50 representative secondary metabolites. All extracts were then analyzed by the Quanlynx software. For metabolite identification, each peak was matched against an internal reference standard database (~800 compounds) as well as tentatively identified by searching the accurate mass in the 34,392 compounds in Antibase 2008 (Laatsch, 2008), comparing UV–VIS data, fragmentations, ionization efficiency in ESI^- versus ESI^+ and the retention time to information in the databases.

2.7. DNA extraction, PCR amplification and sequencing

For DNA analysis, each strain was inoculated in three points onto a PCA plate and incubated as mentioned above. DNA was extracted from 7-day-old PCA cultures with UltraClean Microbial DNA isolation kit (Mo Bio Laboratories, Solana Beach, CA, USA) according to manufacturer's protocol and stored at −20 °C. Amplifications of the three target genes were performed with the following primer combinations: ITS: V9G (de Hoog and Gerrits van den Ende, 1998) and ITS4 (White et al., 1990): *gpd*: gpd1 and gpd2 (Berbee et al., 1999), *tef-1α*: EF1–645F: (TCG TCG TYA TCG GMC ACG TCG A) and EF1–1190R (TAC CAG TGA TCA TGT TCT TGA TGA). EF1–645F and EF1–1190R were designed by aligning sequences of *Gibberella zeae* (XM388987), *N. crassa* (D45837), *Aspergillus fumigatus* (XM745295) and *Ustilago maydis* (XM751978) from GenBank. The numbers of the primers refer to the nucleotide position in *N. crassa* (D45837) at the 3′-end as done previously (Carbone and Kohn, 1999). ITS and *gpd* PCR reactions were performed in 12.5 μl volumes containing 0.5 μl DNA, 1 × NH_4^+-buffer [160 mM $(NH_4)_2SO_4$, 670 mM Tris–HCl (pH 8.8 at 25 °C), 0.1% Tween-20] (Bioline, London, UK), 1 mM $MgCl_2$, 0.04 mM dNTPs, 0.2 pmol of each primer and 0.5 U BIOTAQ™ DNA Polymerase (Bioline, London, UK). *Tef-1α* PCR reactions were performed with 0.8 pmol of each primer and 2.5 mM $MgCl_2$ and with the same concentrations of the remaining ingredients as for ITS and *gpd*. All PCR amplifications were performed after the same scheme with an initial denaturation at 94 °C for 5 min followed by 40 amplification cycles of 94 °C for 30 s, annealing for 30 s and 72 °C for 1:20 min, and a final extension at 72 °C for 7 min. Annealing temperatures were: 48 °C (ITS), 52 °C (*tef-1α*) and 59 °C (*gpd*). Amplicons were run on 1% agarose gels and visualised with UV after ethidium bromide staining. Sequence reactions were performed with the BigDye® Terminator v1.1 Cycle Sequencing Kit (Applied Biosystems, Foster City, CA). All sequence-PCR reactions were performed with the same protocol: 94 °C for 1 min, followed by 30 cycles of 94 °C for 10 s, 50 °C for 5 s and 60 °C for 4 min. DNA was purified with Sephadex® G-50 (Pharmacia-Amersham) and sequenced. All sequences determined in this study have been submitted to GenBank and accession numbers are listed in Table 2.

2.8. Data treatment of molecular sequences

Sequence electrophorograms of forward and backward runs were combined, analyzed, edited using DnaStar SeqMan II (LaserGene). Sequence data were saved and aligned with BioNumerics (Applied Maths, Kortrijk, Belgium). The alignments of *tef-1α*, ITS and *gpd* were concatenated into one alignment to construct a phylogenetic tree. The program RaxML (http://www.phylo.org/portal/Home.do) was used to create the best tree using maximum likelihood and to calculate bootstrap values (Stamatakis et al., 2008). The same program and conditions were used to create individual trees of all three markers used in this study. Genetic diversity of

Table 2
Ascoma production on PCA and growth at 37 °C on PDA together with *gpd* haplotypes and GenBank accession numbers.

#[a]	Genus (species/group)	Ascoma production		Growth at 37 °C	*gpd*	ITS	*gpd*	*tef-1α*
		1. Trial	2. Trial		Haplotype			
1	*Alternaria infectoria* sp.–grp.	+	+	+	1	FJ214885	FJ214836	FJ214932
2	*A. triticina* T (inf–grp)	–	–	+	3	AY762948	FJ214846	FJ214942
3	*A. infectoria* T (inf–grp)	+	–	–	2	FJ214897	FJ214850	FJ214946
4	*A. oregonensis* T (inf–grp)	+	–	+	4	AY762947	FJ214849	FJ214945
5	*A. photistica* T (inf–grp)	–	+	–	nt	FJ214900	FJ214854	FJ214950
6	*A. ethzedia* T (inf–grp)	+	+	+	5	AY278833	FJ214855	FJ214951
7	*A. metachromatica* T (inf–grp)	–	–	–	6	AY762946	FJ214835	FJ214931
8	*A. triticimaculans* T (inf–grp)	–	–	–	7	AY762949	FJ214834	FJ214930
9	*A. infectoria* sp.–grp.	+	–	+	21	FJ214890	FJ214841	FJ214937
10	*A. infectoria* sp.–grp.	+	–	–	22	FJ214886	FJ214837	FJ214933
11	*A. infectoria* sp.–grp.	+	–	–	22	FJ214859	FJ214808	FJ214904
12	*A. intercepta* T (inf–grp)	+	–	+	8	FJ214882	FJ214831	FJ214927
13	*A. viburni* T (inf–grp)	+	–	+	9	FJ214876	FJ214825	FJ214921
14	*A. arbusti* T (inf–grp)	–	–	+	10	FJ214857	FJ214806	FJ214902
15	*A. infectoria* sp.–grp.	+	+	+	11	FJ214887	FJ214838	FJ214934
16	*A. infectoria* sp.–grp.	+	+	–	12	FJ214863	FJ214812	FJ214908
17	*A. infectoria* sp.–grp.	+	+	–	2	FJ214865	FJ214814	FJ214910
18	*A. infectoria* sp.–grp.	+	–	+	13	FJ214866	FJ214815	FJ214911
19	*A. infectoria* sp.–grp.	+	+	–	9	FJ214868	FJ214817	FJ214913
20	*Chalastospora cetera* T	nt[b]	–	–	nt	FJ214864	FJ214813	FJ214909
21	*A. malorum*	nt	–	+	nt	FJ214888	FJ214839	FJ214935
22	*A. malorum*	nt	–	+	nt	FJ214870	FJ214819	FJ214915
23	*A. malorum*	nt	+	+	nt	FJ214894	FJ214845	FJ214941
24	*A. malorum*	nt	+	+	nt	FJ214861	FJ214810	FJ214906
25	*A. malorum*	nt	–	+	nt	FJ214860	FJ214809	FJ214905
26	*A. malorum* var. *polymorpha*	nt	–	+	nt	FJ214883	FJ214832	FJ214928
27	*A. malorum*	nt	+	+	nt	FJ214884	FJ214833	FJ214929
28	*A. malorum*	nt	–	+	nt	FJ214895	FJ214847	FJ214943
29	*A. malorum*	nt	–	+	nt	FJ214896	FJ214848	FJ214944
30	*Embellisia abundans*	nt	–	–	nt	FJ214898	FJ214851	FJ214947
31	*E. abundans* T	nt	–	–	nt	AB120848	FJ214852	FJ214948
32	*A. infectoria* sp.–grp.	nt	–	–	6	FJ214872	FJ214821	FJ214917
33	*A. infectoria* sp.–grp.	nt	–	+	23	FJ214873	FJ214822	FJ214918
34	*A. infectoria* sp.–grp.	nt	+	+	24	FJ214862	FJ214811	FJ214907
35	*A. infectoria* sp.–grp.	nt	+	+	15	FJ214880	FJ214829	FJ214925
36	*A. infectoria* sp.–grp.	nt	–	+	15	FJ214867	FJ214816	FJ214912
37	*A. infectoria* sp.–grp.	nt	+	+	15	FJ214871	FJ214820	FJ214916
38	*A. infectoria* sp.–grp.	nt	+	–	9	FJ214875	FJ214824	FJ214920
39	*A. infectoria* sp.–grp.	nt	–	+	15	FJ214881	FJ214830	FJ214926
40	*A. infectoria* sp.–grp.	nt	–	+	19	FJ214877	FJ214826	FJ214922
41	*A. infectoria* sp.–grp.	nt	–	+	9	FJ214879	FJ214828	FJ214924
43	*A. infectoria* sp.–grp.	nt	nt	nt	2	FJ214892	FJ214843	FJ214939
44	*A. infectoria* sp.–grp.	nt	–	+	20	FJ214878	FJ214827	FJ214923
45	*A. infectoria* sp.–grp.	nt	–	–	14	FJ214856	FJ214805	FJ214901
46	*A. infectoria* sp.–grp.	nt	–	+	15	FJ214899	FJ214853	FJ214949
47	*A. infectoria* sp.–grp.	nt	+	–	6	FJ214858	FJ214807	FJ214903
48	*A. infectoria* sp.–grp.	nt	nt	nt	16	FJ214889	FJ214840	FJ214936
49	*A. infectoria* sp.–grp.	nt	nt	nt	17	FJ214869	FJ214818	FJ214914
50	*A. infectoria* sp.–grp.	nt	nt	nt	15	FJ214874	FJ214823	FJ214919
51	*A. infectoria* sp.–grp.	nt	nt	nt	18	FJ214891	FJ214842	FJ214938
52	*A. infectoria* sp.–grp.	nt	nt	nt	15	FJ214893	FJ214844	FJ214940

[a] Analysis number in this study. #42 is not included.
[b] Not tested.

aligned sequences and the standardized Index of Association (I_A^s) was calculated with LIAN 3.5 (Haubold and Hudson, 2000) by combining clustering information of the individual trees. The phylogenetic network was created with SplitsTree v4.8. The network structure was based on the neighbornet algorithm with a threshold set to 10^{-4} and applying the LogDet transformation. LogDet is a distance transformation that corrects for biases in the base composition (Wägele and Mayer, 2007). The *phi*-test incorporated in the SplitsTree software (Huson and Bryant, 2006) was used to test signals of recombination ($p < 0.05$, significant evidence of recombination). The test is proven to be a robust calculation and no previous knowledge about population history, recombination rate, mutation rate and rate heterogeneity across sites (Bruen et al., 2006) is necessary. Although large splits in networks do not necessarily imply recombination, split decomposition networks in conjunction with the *phi*-test can easily detect which sequences in a given data set contribute the most to the recombination signal (Salemi et al., 2008). The *phi*-test is repeated after possible recombinants are deleted from the alignment until $p > 0.05$ (no evidence of recombination). DnaSP v4.5 (Rozas and Rozas, 1995) was used to find the different haplotypes in the *gpd* alignment. Gaps and missing data were not considered during calculation.

3. Results

3.1. Morphology

Examination of the sporulation patterns on PCA after seven days of growth in alternating light showed three different and very distinct morphologies as shown in Fig. 1. *A. malorum*, *A. malorum* var.

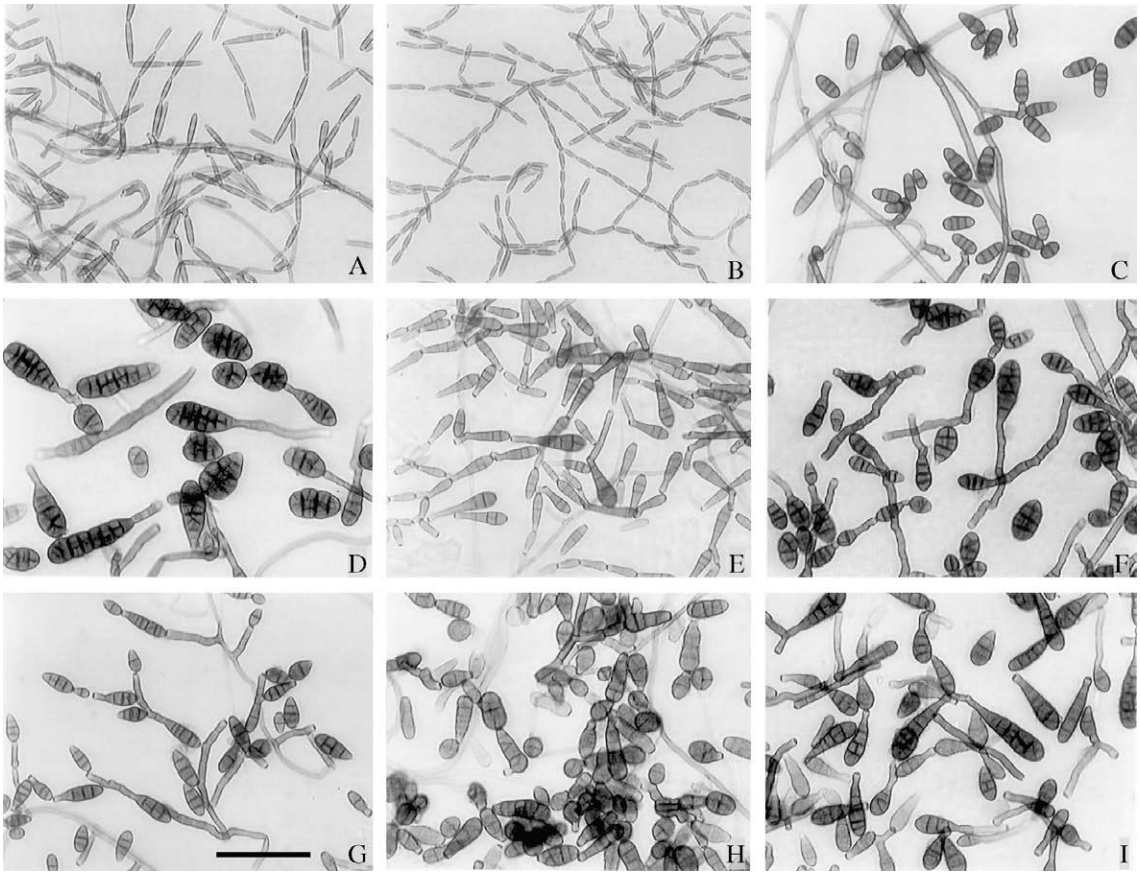

Fig. 1. Morphology plates. (A): *Chalastospora cetera* (#20), (B): *Alternaria malorum* (#25), (C): *Embellisia abundans* (#31) and six strains belonging to the *A. infectoria* species–group: (D): *A. oregonensis* (#04), (E): *A. infectoria* (#03), (F): *A. arbusti* (#14) and (G–I): three *A. infectoria* species–group strains (#32, #44 and #17, respectively). Bar in *G* = 50 μm.

polymorpha and *C. cetera* all had cylindrical didymo- and phragmoconidia produced in very long branching chains (Fig. 1A and B). Both strains of *E. abundans* had solitary, ovoid phragmoconidia (Fig. 1C), while all strains of the *A. infectoria* species–group shared the same morphology: ovoid, obpyriform or obclavate phragmo- and dictyoconidia with secondary conidiophores of varying length produced in branched chains (Fig. 1D–I). Type cultures fitted the descriptions, except *A. arbusti* (#14), which, under the growth conditions in this study, showed a more branched three-dimensional structure than the original description depicted (Simmons, 2007). Conidial sizes, shapes, ornamentation, color etc. varied greatly between strains, whereas conidial appearance was quite consistent within a strain: e.g. conidia of *A. infectoria* (#03) were smooth, narrow-obpyriform and sallow colored (Fig. 1E), while conidia of *A. infectoria* species–group (#44) were narrow-obpyriform to broad-ovoid, finely rough and bronze colored (Fig. 1H). None of the strains morphologically identified as belonging to the *A. infectoria* species–group could be assigned to any of the type cultures and no two strains, except *A. infectoria* species–group strains (#10 and #11), could be classified as belonging to the same taxon.

Table 2 shows the production of proascomata (ascomata without mature ascospores) after 6 months of incubation on PCA at 7 °C. In the first trial, where three strains were inoculated on the same PCA plate, no mating between strains was observed. Proascomata (Fig. 2) were formed in the center of each colony and in areas in the agar furthest away from the two other colonies and there was a clear demarcation line between colonies. In the second trial, where the same strain had been inoculated twice on the same plate, proascomata were again formed at the center and furthest away from the other colony. Fourteen out of nineteen *A. infectoria* species–group strains produced proascomata in the first trial, and only seven of these in the second trial. Additional 14 strains were tested in the second trial, out of which five produced proascomata. In the second trial, neither *C. cetera* nor *E. abundans* produced proascomata, but three out of the nine *A. malorum* did. In contrast to the strains of the *A. infectoria* species–group, the three *A. malorum* strains produced their proascomata on the toothpicks and not in the agar. When the experiment was terminated after 6 months, none of the proascomata had yielded any matured ascospores.

3.2. Growth on different media

The result of the experiment on PDA at 37 °C given in Table 2 showed that 28 out of the 45 tested strains were able to grow at this temperature. Unfortunately, it was not possible to test all 51 strains in the set, since six strains were not viable after the first chemical experiments. Table 2 shows that all nine *A. malorum* strains were able to grow at 37 °C, but not *C. cetera*. During the incubation period, the colonies of *A. malorum* became dark brown and the mycelium thinner and more thread-like. Of the 33 tested strains of *A. infectoria* species–group, 20 were able to grow at 37 °C. The colonies lost their aerial mycelium, became waxy in their growth, and only produced filamentous mycelium after they were taken out of the 37 °C incubator. The only viable strain of *A. infectoria* species–group from a human infection (#45) was not able to grow on PDA at 37 °C.

Examination of the colony appearance on DRYES incubated at 25 °C showed that most of the 51 strains produced hairy to granu-

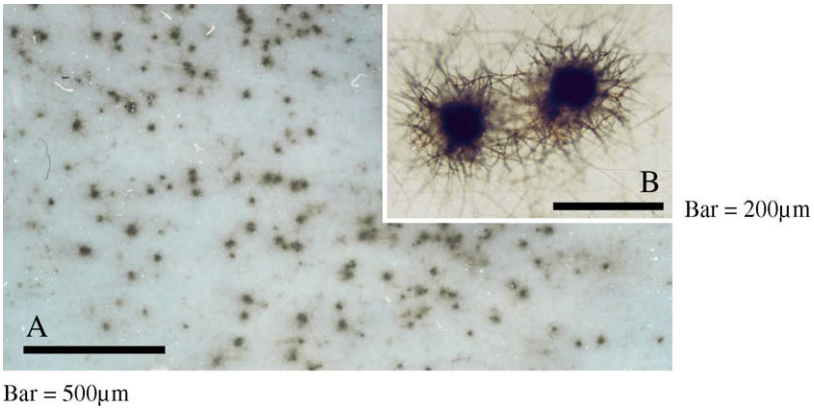

Fig. 2. Proascomata in 3-week-old PCA cultures. (A): *Alternaria infectoria* species–group #19 (bar = 500 µm) and (B): *A. infectoria* species–group #16 (bar = 200 µm).

lar mycelium, whitish to grayish in color. Some of the *A. infectoria* species–group strains produced only wet, yeast-like colonies on DRYES, especially the strains isolated from human lesions, which, however, did not affect their metabolite production. Filamentous mycelium was produced when the strains were transferred to PDA or PCA. Sporulation of the *A. infectoria* species–group was only seen on PCA and sometimes scarification and prolonged incubation were needed, while *A. malorum, C. cetera* and *E. abundans* sporulated well on PCA as well as on PDA + DN and PDA. DRYES and DG18 did not accommodate any sporulation. As a curiosity, it should be mentioned that *A. metachromatica* (#07) on PDA + DN produced an extracellular pigment that turned the reverse of the plate dark blue.

3.3. Chemical classification

The chemical HPLC-UV–VIS analyses of the three growth media, DRYES, DG18 and PDA + DN, showed that the metabolite production, qualitative as well as quantitative, was greatest on DRYES and that metabolite production seemed to be inhibited on PDA + DN. Fig. 3 shows six selected HPLC chromatograms made from the DRYES extracts.

Automated and unbiased chemical image analyses (CIA) of the HPLC-UV–VIS files were made with extracts from all three growth media to aid the selection of species-specific metabolites (dendrograms not shown). All three dendrograms gave the same grouping, but the one made with extracts from DRYES gave the most detailed dendrogram. It showed that the 51 strains grouped in four major clusters. One cluster contained all eight *A. malorum* strains, the *C. cetera* (#20) strain, and the type culture of *E. abundans* (#31). A second cluster contained 13 *A. infectoria* species–group strains, including the type cultures of *A. infectoria* (#03), *A. ethzedia* (#06), and *A. metachromatica* (#07), together with *E. abundans* (#30) and *A. malorum* var. *polymorpha* (#26). A third cluster contained 10 *A. infectoria* species–group strains, including the type cultures of *A. intercepta* (#12) and *A. viburni* (#13), while the last cluster contained 12 *A. infectoria* species–group strains, including type cultures of *A. photistica* (#05), *A. arbusti* (#14), *A. oregonensis* (#04), *A. triticina* (#02) and *A. triticimaculans* (#08). Visual examination of the HPLC chromatograms of *E. abundans* (#30) and *A. malorum* var. *polymorpha* (#26) showed very few peaks, meaning a very low metabolite production. The location of these two stains in the dendrogram was therefore questionable and they where subsequently removed from further analyses.

A binary matrix was made by visual examination of each peak and its associated UV–VIS spectrum in the HPLC chromatograms and the CIA dendrograms. On no occasion were there metabolites produced on DG18 or PDA + DN that were not found in DRYES, however, some metabolites were easier to detect on DG18 due to a qualitatively simpler metabolite profile. The matrix consisted of 137 recognizable metabolites for the 51 strains and was subjected to a Partial Least Squares Regression (PLS-R) (result not shown), which gave metabolites specific for the *A. malorum* strains, the *C. cetera* strain, the *A. infectoria* species–group strains and the *E. abundans* strains, respectively (see Table 3). All 51 chromatograms were analyzed for the production of known *Alternaria* metabolites and tested negative for AAL-toxins, alternariols, altersolanols, altenuenes, tentoxin and tenuazonic acid. On the other hand, HPLC-UV–VIS as well as HPLC-MS analyses showed that all 51 strains, including *E. abundans* (#30) and *A. malorum* var. *polymorpha* (#26), were able to produce infectopyrone and 4*Z*-infectopyrone. Altertoxin derived metabolites were restricted to the *A. infectoria* species–group, but not produced consistently throughout the species–group, while macrosporin was found in three *A. malorum* strains. Novae-zelandin production was shared by *E. abundans* and the *A. infectoria* species–group, but again not produced consistently throughout the species–group. *A. malorum* and *C. cetera* had a number of metabolites of unknown structure in common (e.g. RI value 694), but also produced unknown metabolites specific to each species (e.g. RI values 715 and 894, respectively). *E. abundans* did not produce any known metabolites, except for the infectopyrone, 4*Z*-infectopyrone, and novae-zelandin A, and only few species specific metabolites (e.g. RI values 691 and 779a) were detected.

Based on the combined results of the CIA and the PLS-R, a matrix that consisted of 49 strains [excluding *E. abundans* (#30) and *A. malorum* var. *polymorpha* (#26)] and 124 known and unknown metabolites (excluding infectopyrones and other consistently produced metabolites) was constructed. The matrix was subjected to cluster analysis and the resulting dendrogram is shown in Fig. 4. The dendrogram shows a division of the 49 strains into two clusters, A (in light grey) and B. Cluster A contains the type culture of *E. abundans* (#31), the type culture of *C. cetera* (#20) together with six *A. malorum* strains in sub-cluster A1 and two *A. malorum* strains (#22 and #28) in sub-cluster A2. Cluster B, holding all the 39 strains of the *A. infectoria* species–group, could be divided into two sub-clusters with type cultures of *A. photistica* (#05) and *A. triticina* (#02) as outliers. Sub-cluster B1 contained six *A. infectoria* species–group strains and the type cultures of *A. triticimaculans* (#08), *A. intercepta* (#12) and *A. viburni* (#12) (marked with ♦), while the majority of the *A. infectoria* species–group strains clustered closely together in sub-cluster B2. Both B sub-clusters could be further divided based on production of different metabolites. The color-coding of strains in Fig. 4 is referring to different haplotypes.

The result of a principal component analysis of the 39 *A. infectoria* species–group strains and 79 metabolites (given as their RI

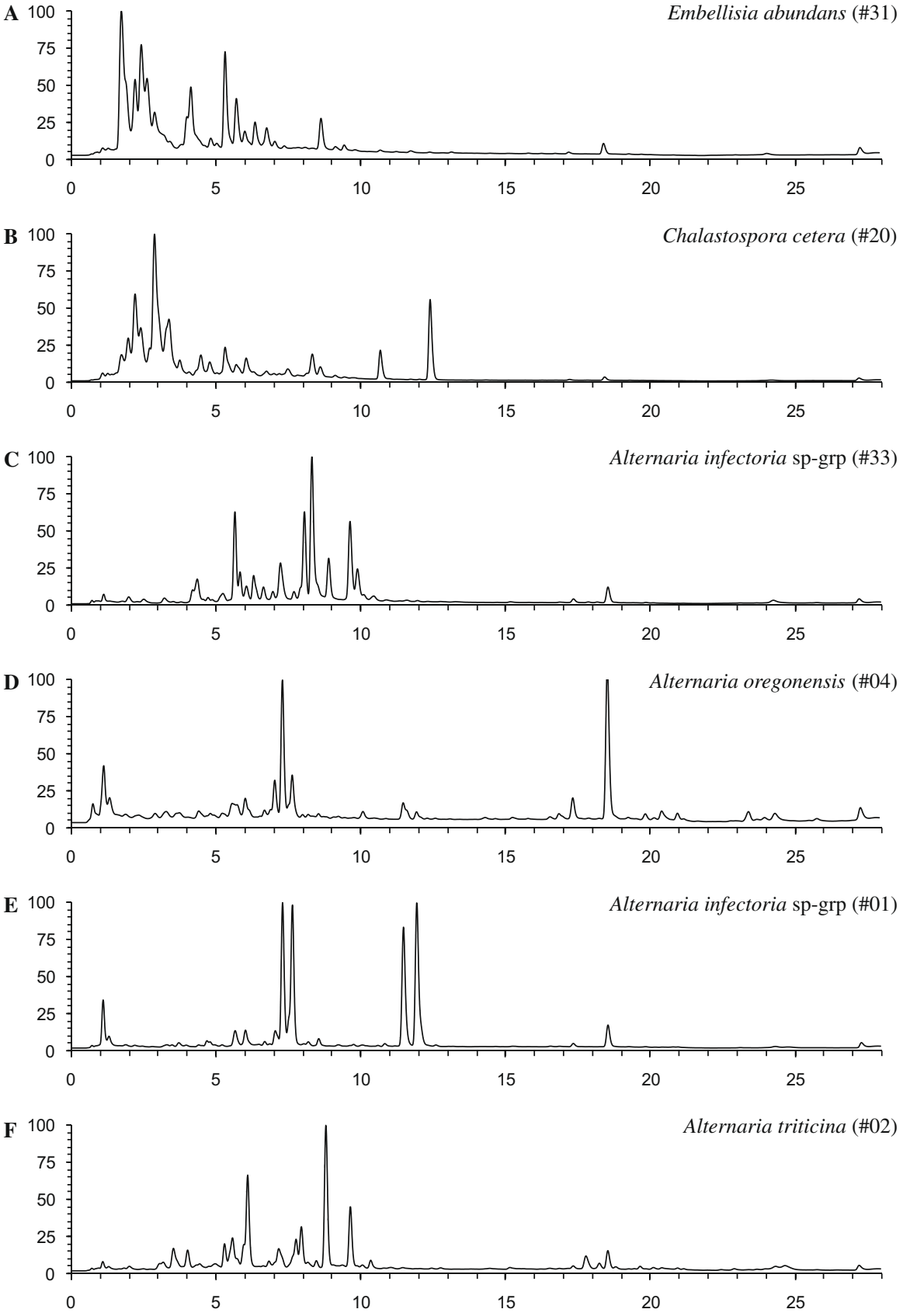

Fig. 3. HPLC chromatograms (wave length 210 nm). (A): *Embellisia abundans* (#31), (B): *Chalastospora cetera* (#20) and four strains belonging to the *Alternaria infectoria* species group; (C): *A. infectoria* species–group (#33), (D): *A. oregonensis* (#04), (E): *A. infectoria* species–group (#01) and (F): *A. triticina* (#02).

values) is shown in Fig. 5. It shows the association between metabolites and the strains that produce them. Metabolites common to most strains are located in the center, while metabolites specific to a few strains are located around the perimeter together with

Table 3
Production of known metabolites and selected, unknown metabolites, given by their retention index (RI) value, from *Alternaria infectoria* species–group, *A. malorum*, *Chalastospora cetera* and *Embellisia abundans*.

Metabolite (RI)[a]	*A. infectoria* sp–grp (39)	*A. malorum* (9)	*C. cetera* (1)	*E. abundans* (2)
Altertoxin derived (855)[b]	31	–	–	–
Altertoxin derived (820)	9	–	–	–
Altertoxin derived (846)	4	–	–	–
Infectopyrone (839)[c]	39	9	1	2
4Z-Infectopyrone (824a)	39	9	1	2
Infectopyrone derived (706)	30	2	–	–
Infectopyrone derived (713b)	23	1	–	–
Macrosporin (1068)	–[f]	3	–	–
Novae-zelandin B (892)	29	–	–	–
Novae-zelandin A (680a)	19	–	–	2
Novae-zelandin derived (726)	6	–	–	–
569	19	–	–	–
950[d]	13	–	–	–
691	–	–	–	1
779a	–	–	–	1
715	–	5	–	–
894	–	–	1	–
694	–	7	1	–
1010	–	4	1	–
642	–	7	1	1
1120	–	6	1	1
1076[e]	39	7	1	2
1047	35	5	1	1
752	26	5	–	1

[a] RI: retention index value, calculated by the HPLC from retention time.
[b] Same as metabolite 3 in Andersen and Thrane (1996).
[c] Same as metabolite 2 in Andersen and Thrane (1996).
[d] Same as metabolite 5 in Andersen and Thrane (1996).
[e] Same as metabolite 6 in Andersen and Thrane (1996).
[f] Not detected.

the strains producing them. From Fig. 5 it can be seen that strains in sub-cluster B1 in Fig. 4 (marked with ♦) produced a large number of metabolites including the altertoxins and novae-zelandins, whereas strains in sub-cluster B2 produce fewer metabolites and not altertoxins or novae-zelandins. On the other hand, strains in B2 produce metabolites of unknown structure (e.g. RI values 569, 706, 713b, 752, 813), which are not produced by strains in B1. In general, many individual metabolites of unknown structure were found to be specific to only one or a few strains in the *A. infectoria* species–group, which hampered a clear grouping.

3.4. Molecular cladification

The obtained sequences of *gpd* were 444–446 bp for *A. photistica* and the *A. infectoria* species–group and of 424 bp for *A. malorum*, *E. abundans,* and *C. cetera.* The aligned *gpd* sequences contained one intron of approximately 114 bp. The alignment dataset of all the strains contained 456 bp with 131 variable sites of which 85 were parsimony informative. Sequences of *tef-1α* were 437–440 bp containing two introns of approximately 250 bp in total. The *tef-1α* alignment dataset consisted of 443 bp containing 113 variable sites of which 65 were parsimony informative. The obtained ITS sequences were 490 bp for *A. photistica*, 519–525 bp for the *A. infectoria* species–group strains, 533–534 bp for the *A. malorum* strains and 523 bp and 525 for the *E. abundance* and *C. cetera* strains, respectively. The ITS sequence for *A. photistica* was smaller than those of the remaining strains due to a major deletion in ITS1. The ITS alignment dataset of all the strains contained 544 bp with 106 variable sites of which 60 were parsimony informative. The ITS and *tef-1α* dendrograms gave the same major division as the *gpd* dendrogram, but with lower resolution (data not shown). Strains that were identical in one gene sequence were nearly always different in another. Molecularly, all the *A. infectoria* species–group strains were mutually similar, but never identical, except for *A. infectoria* species–group strains (#10 and #11), which have identical sequences in all three tested genes.

Fig. 6 shows an unrooted dendrogram for all 51 strains of the concatenated ITS, *tef-1α* and *gpd* sequences using maximum likelihood in RaxML. It shows two major clades, one with 38 *A. infectoria* species–group strains and with *A. triticina* (#02), three strains of *A. infectoria* species–group (#09, #48 and #51) and *A. photistica* as outliers and another clade with all *A. malorum*, *C. cetera* and *E. abundans* strains (in light grey). Within the latter clade, *A. malorum* var. *polymorpha* (#26) could not be distinguished from the remaining eight *A. malorum* strains. Nearest neighbors of *A. malorum* were *C. cetera* and *E. abundans*. The degree of variability within the *A. infectoria* species–group proved to be limited in all genes.

Fig. 7 shows the nucleotide differences between 38 strains in the *A. infectoria* species–group [excluding *A. photistica* (#05)]. As seen in Fig. 7, most nucleotide differences in the three genes were observed in the spacers and introns, although there were some mutations in the coding region of *gpd*, which all occurred on the third codon position often with a silent C to T substitution. Table 4 shows alignment data for the three genes. Internal ITS alignment of the 38 strains in the *A. infectoria* species–group resulted in 40 variable sites of which 35 were parsimony informative and located in either the ITS1 or ITS2. The *tef-1α* alignment resulted in 113 variable sites of which 53 were parsimony informative. The *gpd* alignment showed 109 variable and 59 parsimony informative sites of which 18 were located in the 114 bp intron.

Using DnaSP on the *gpd* alignment data of the 38 strains in the *A. infectoria* species–group, haplotypic groups were defined and are given in Table 2. Most haplotypic groups contained only one strain except for haplotype 2 (#3, #17 and #43), haplotype 6 (#7, #32 and #47), haplotype 9 (#13, #19, #38 and #41), haplotype 15 (#35–37, #39, #46, #50 and #52) and haplotype 22 (#10–11), resulting in 24 distinct haplotype groups. Fig. 8 shows the haplotype network. The standardized Index of Association (I_A^S) of the

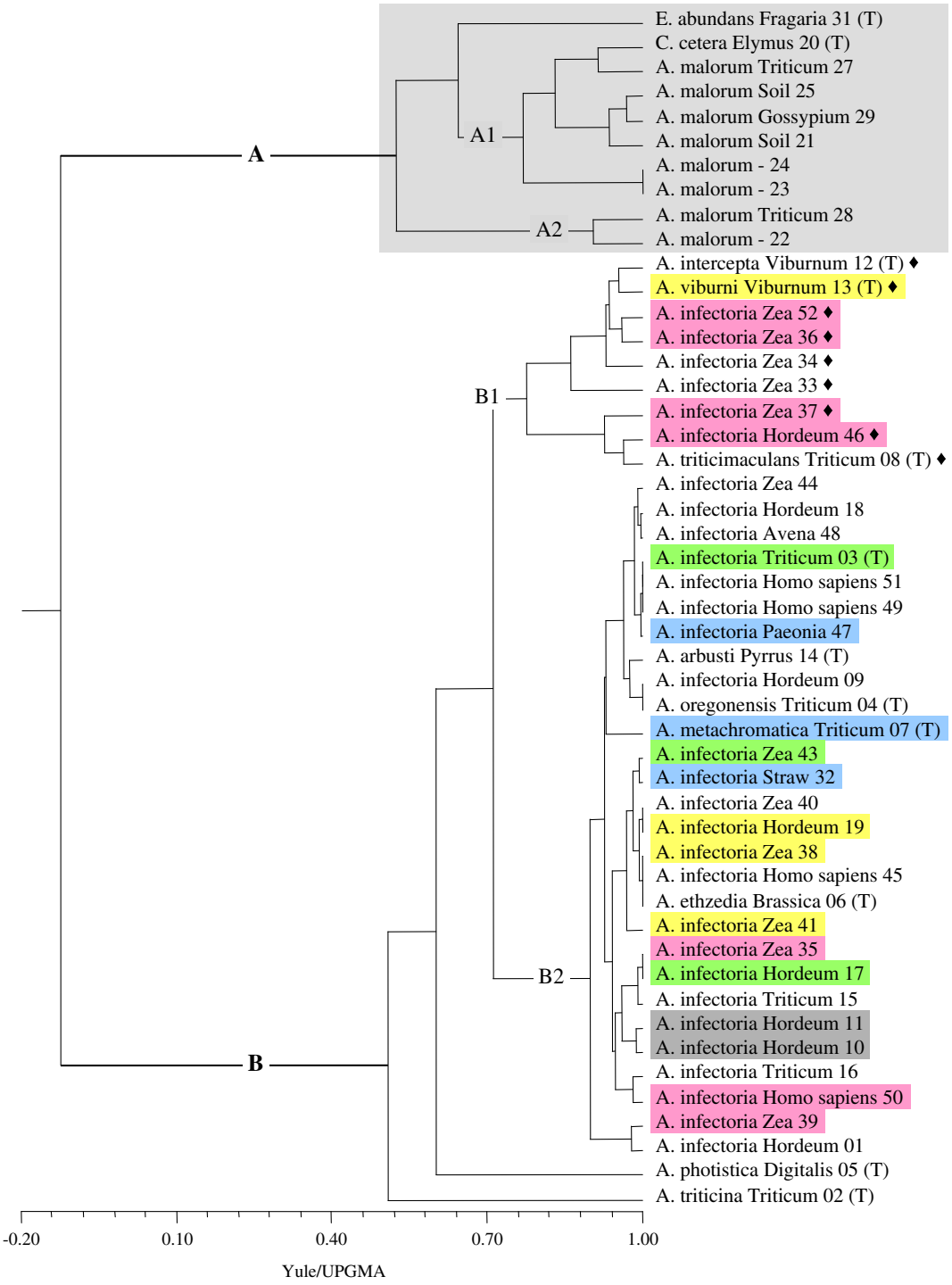

Fig. 4. Dendrogram based on a cluster analysis of 49 metabolite profiles (1 *Embellisia abundans*, 1 *Chalastospora cetera*, 8 *Alternaria malorum* and 39 strains belonging to the A. *infectoria* species–group). Color-coding in the B cluster corresponds to haplotype groups given in Table 2 and Fig. 8. Strain labels: strain ID/host/strain number/type culture. Dendrogram calculated using the Yule correlation coefficient and UPGMA as the clustering method. Axis shows the correlation coefficient from −1 to 1.

same *A. infectoria* species–group strains showed a tendency towards recombination events, $(I_A^S) = 0.1627$. LIAN v3.5 was used to calculate the standardized Index of Association with 1,000,000 Monte Carlo samplings. The neighbornet splitstree of *gpd* alignment data (not shown) of the *A. infectoria* species–group showed mostly a treelike structure. The network also showed conflicting phylogenetic trees (histories) that can not be shown with a bifurcating tree. Conflicting phylogenetic signals can occur by recombination or by convergent substitutions and can not be distinguished by looking at the network alone (Salemi et al., 2008). However, a *phi*-test was able to detect the presence of recombination in aligned sequences. Repeated *phi*-test calculations after removing single sequences from the alignment showed the presence of recombinants. When the *p*-value increased till 0.05 or more, it was obvious that the recombinants were deleted from the alignment. Table 4 shows the *p*-values for the three genes in the *phi*-test of the 38 *A. infectoria* species–group strains [excluding *A. photistica*]. ITS and *tef-1α* had *p*-values > 0.05, which indicated

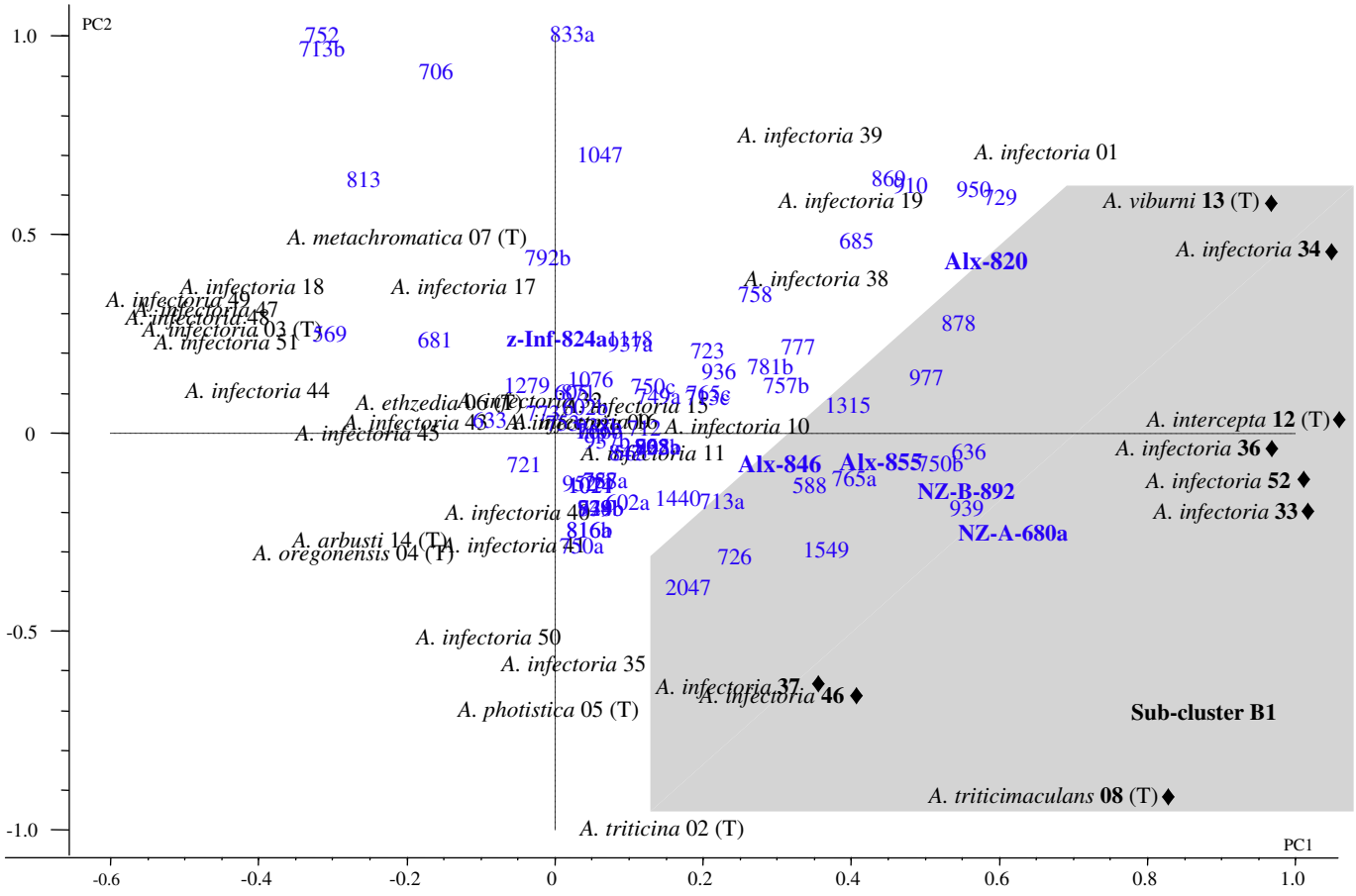

Fig. 5. Loadings plot based on a principal component analysis of 79 individual metabolites (39 strains belonging to the *A. infectoria* species–group). Strains are in black and metabolites in blue. Metabolites of known structure: Alx: altertoxin derivatives; NZ: novae-zelandin derivatives; z-Inf: infectopyrone derivate. Metabolites of unknown structure are only given by their Retention Index (RI) values calculated from their retention time on HPLC. Strain labels: strain ID/strain number/type culture. Strains in the grey box marked with ♦ correspond to sub-cluster B1 in Fig. 4. Axes are score values.

the absence of recombination. However, the *p*-value of *gpd* was 7.5×10^{-4} suggesting the presence of recombination events in this gene. After deleting strains #08, #45 and #51 (CBS 578.94, CBS 102692 and CBS 110804, respectively), the *phi*-test showed no significant evidence of recombination in the *gpd* data ($p > 0.05$) and therefore these three strains were considered to be recombinants.

4. Discussion

At genus level, the *Alternaria infectoria* species–group could clearly be separated from the *A. malorum/C. cetera/E. abundans* group based on morphology as well as chemical classification and molecular cladification. The results show that strains morphologically identifiable as *A. infectoria* species–group produced altertoxins and novae-zelandins and yielded ITS, *gdp* and *tef-1α* sequences that were different from those of the *A. malorum/C. cetera/E. abundans* group (Figs. 1, 4 and 6 and Table 3). *E. abundans*, on the other hand, could only be segregated from the *A. malorum/C. cetera* group by morphology (Fig. 1), but not with any confidence by molecular or chemical means. Besides, the chemical similarity turned out to be too large and the number of species/strains used proved to be too few to speculate on the placement of *Embellisia*, compared to *A. malorum/C. cetera* group. Other studies based on ITS, SSU and *gpd* data, show species of *Embellisia* are scattered among genus *Alternaria* as well as genus *Ulocladium* despite its distinct morphology (Pryor and Bigelow, 2003). In contrast, *C. cetera* could not be segregated from the *A. malorum*/*A. malorum* var. *polymorpha* group by morphological, molecular, or chemical means (Figs. 1, 4 and 6 and Table 3). Two *A. malorum* strains (#23 and #24) were distinct and identical in all three methods. The other *A. malorum* strains yielded metabolite profiles that were similar, but not identical to each other and to that of *C. cetera*. Morphologically, *A. malorum* and *C. cetera* showed the same general sporulation pattern, but with some variation in conidial size and septation. The polyphasic data in this study shows that *A. malorum* var. *polymorpha* and the eight *A. malorum* strains, do not belong in the *A. infectoria* species–group as proposed by Braun et al. (2003), but suggest they belong to the same genus as *Chalastospora cetera*, however, as several distinct species.

The production of infectopyrones and a pair of compounds with unknown structure (RI values 1047 and 1076) by all genera in this study corroborates the close relationship found in the molecular analyses, but on the other hand, some species of *Ulocladium*, which are phylogenetically more related to small-spored *Alternaria* (Pryor and Bigelow, 2003), also produce infectopyrones (Andersen and Hollensted, 2008) and these metabolites may be more widespread in *Pleosporaceae*. Furthermore, this is the first report on the production of infectopyrones by *A. malorum*, *C. cetera*, and *E. abundans* and the production of macrosporin and novae-zelandin A by *A. malorum* and *E. abundans*, respectively.

At species level, the 10 *Alternaria* type cultures representing morphological species within the *A. infectoria* species–group were

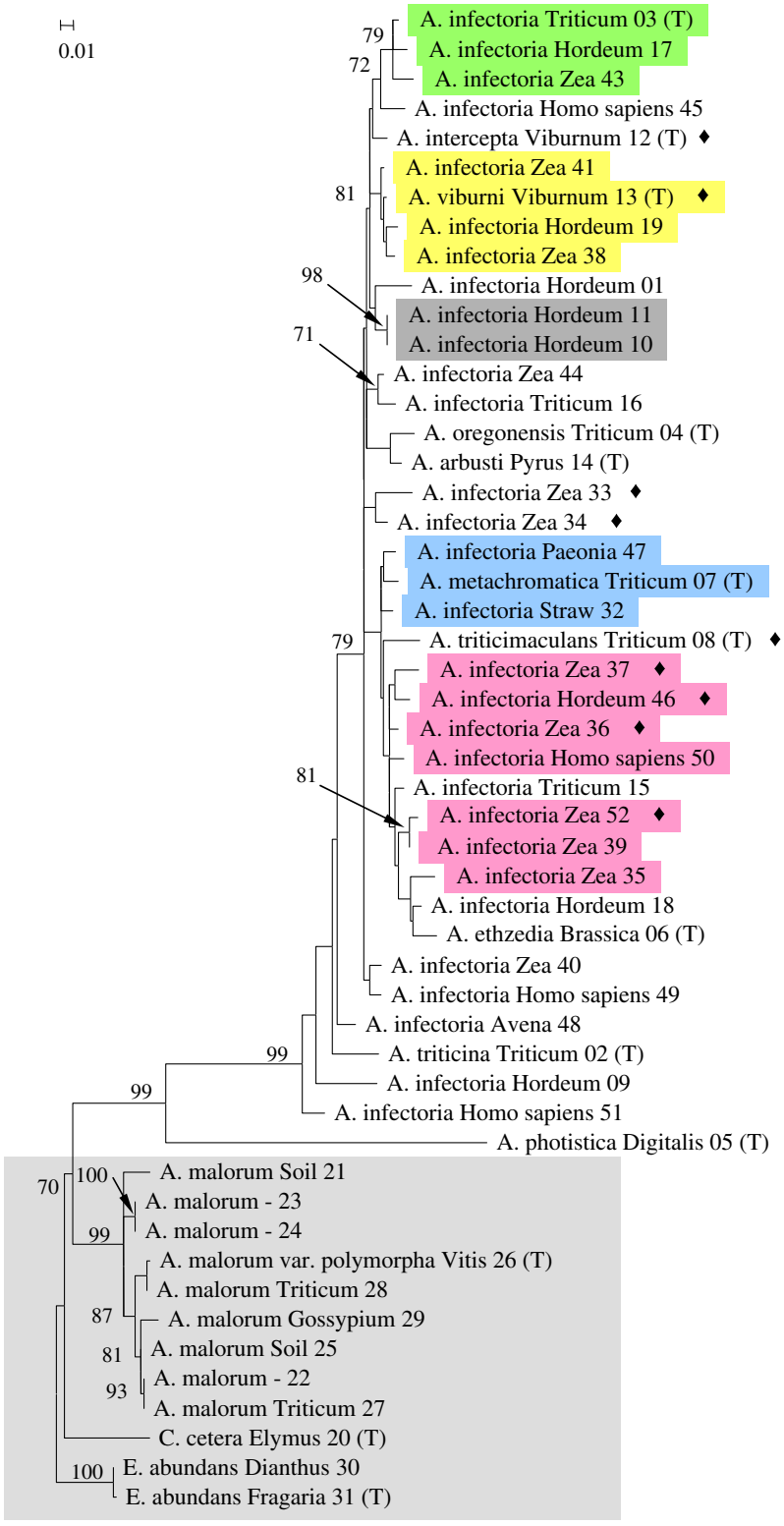

Fig. 6. Unrooted consensus dendrogram based on 51 strains (2 *Embellisia abundans*, 1 *Chalastospora cetera*, 39 *Alternaria infectoria* species–group, 8 *A. malorum* and 1 *A. malorum* var. *polymorpha*). Maximum likelihood tree of 3 partial genes (ITS, *gpd* and *tef-1α*) constructed using RaxML (Cipres webserver). Bootstrap values > 70% are indicated. Color-coding in the *A. infectoria* species-group clade corresponds to haplotype groups given in Table 2 and Fig. 8. Strains marked with ♦ correspond to cluster B1 in the chemical analysis. Strain labels: strain ID/strain number/type culture.

located in different sub-clades depending on the molecular sequence examined, but with *A. photistica* (#05) and *A. triticina* (#02) as outliers. With each individual gene, variability was largely random, judging from low bootstrap values and from obtaining different groupings when different algorithms were used for tree reconstruction. When genes were concatenated, *A. viburni* (#13) clustered at 81% bootstrap support with three strains (#19, #38 and #41) identified as *A. infectoria* species–group *sensu* Simmons.

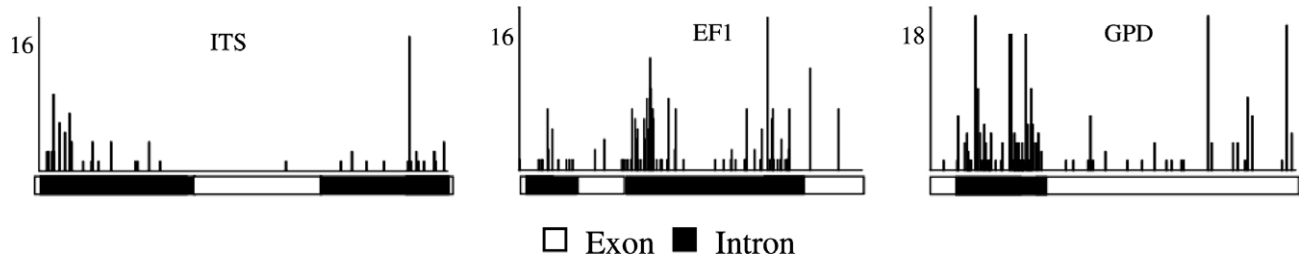

Fig. 7. Mutations at each position in the aligned ITS, *tef-1α* and *gpd* sequences of the 38 *A. infectoria* strains (except *A. photistica* #05) with the predicted exons and introns.

The single type cultures were not unambiguously separated from the core of *A. infectoria*. The same pattern was seen in the chemical data with *A. photistica* (#05) and *A. triticina* (#02) as outliers. No distinct groups or clades were formed in the molecular analyses, while there was a certain grouping in metabolite profiles and metabolite families (Figs. 3–5 and Table 3). Some *A. infectoria* species–group strains were able to produce altertoxin derivatives, while others produced metabolites of unknown structures, but not altertoxins. No distinct morphological groups were seen either among the strains in the *A. infectoria* species–group. Morphology showed that basically each strain was a taxon in its own right. Lastly, no groupings or correlations could be found between proascoma formation, ability to grow at 37 °C, host or geographic origin and haplotypes, metabolite production or morphological identity.

Our original hypothesis was that taxa in *Lewia*/*A. infectoria* species–group were sexual fungi and that molecular sequence analyses and metabolite profiling would yield a number of groups according to the genealogical concordance phylogenetic species recognition (GCPSR) (Taylor et al., 2000). Our data, however, indicate that only three strains in the *A. infectoria* species–group show evidence of recombination and that several isolates are able to produce proascomata in axenic culture. Since several taxa in the *A. infectoria* species–group have been shown to produce ascomata with viable ascospores in axenic cultures (Kwasna and Kosiak, 2003; Simmons, 2007; unpublished results), *Lewia*/*A. infectoria* species–group must, at least in part, be homothallic and the purpose of ascoma formation in nature could be a survival strategy. The high similarity in nucleotide sequence amongst the *A. infectoria* species–group strains (Fig. 6), suggests that most strains are clonal and may have derived via mutations from one common ancestor similar to the arbuscular mycorrhizal fungi (Rosendahl, 2008).

Several studies (reviewed in Taylor et al., 2000; O'Donnell et al., 2004) show an increase in numbers of taxa, when going from morphological species recognition via biological recognition to GCPSR, which corresponded with either geographic origin or hosts. In our study we see the opposite: molecular cladification yields the lowest number of taxa in the *A. infectoria* species–group (*A. photistica* and one phylogenetic taxon), while the chemical classification gives more (*A. photistica* and *A. triticina* and two chemically different taxa) and with morphological appearance giving the highest number (38 morphologically different taxa). Applying GCPSR to the *A. infectoria* species–group would lead to synonymizing of all morphological species in the *A. infectoria* species–group under one name: *A. infectoria* Simmons. Alternatively, morphological species recognition could be applied and strains in the *A. infectoria* species–group would represent new "emerging" species that require a name and a formal description. But according to Taylor et al. (2000) and Rosendahl (2008), GCPSR can only be applied to sexual/heterothallic fungi, not to homothallic/clonal strains, so neither of the two approaches (one species or 38 species) is workable.

In practice, however, there is a regular need for identification of *Alternaria* isolates, because they have acquired different abilities in nature, which affect us negatively. Some isolates have been encountered as opportunistic human pathogens, others as plant pathogens and others again are saprotrophic on cereals producing biologically active metabolites. Artificial identification systems based on any stable differentiation characters (e.g. PCR, AFLP, metabolite profiles, sporulation patterns obtained under standardized conditions) still play an important role in taxonomy. Strains in the *A. infectoria* species–group show characteristic phenotypical traits, which can be detected, recognized, and used for identification. Depending on the users needs, identification of taxa in the *A. infectoria* species–group can be done to different levels. In medical mycology, molecular identification using ITS is fast, well-known and often the only method to obtain the correct diagnosis for isolates in the *A. infectoria* species–group, since strains from human lesions rapidly loose their ability to sporulate *in vitro*. Strains used in this study that originated from human skin lesions sporulated poorly, even under optimal conditions, and went sterile after one or two transfers. However, they still maintained their ability to produce all the characteristic metabolites in spite of their vegetative or yeast-like growth. Concerning alternarioses in humans or animals, generally only identification to species–group level is needed, since the same medical treatment (e.g. itraconazole) is likely to be applicable regardless of taxon identification within the *A. infectoria* species–group (Brasch et al., 2008; Dye et al., 2009). In plant pathology, phytosanitary, and quarantine, on the other hand, ITS sequencing is not enough to identify a known pathogen or discover a new pest that requires quarantine. With our current knowledge, described plant pathogens like *A. triticina*, *A. viburni,* and *A. intercepta* can be distinguished from other taxa of the *A. infectoria* species–group using morphology. In the cladistic analyses, *A. triticina* (#02) grouped with different taxa in the *A.*

Table 4
Alignment data set for 38 strains in the *Alternaria infectoria* species–group, except *A. photistica,* of the three genes with number of mutations, parsimony informative mutations, sites and *p*-value in *phi*-test.

	Total number of sites (gaps/missing)	Total number of mutations	Number of parsimony informative sites	Parsimony informative mutations (%)[a]	Parsimony informative sites (%)[b]	*phi*-Test *p*-value[c]
gpd	456 (40)	109	59	54.1	12.9	$7.5 \cdot 10^{-4}$
tef-1α	443 (17)	113	53	46.9	12.0	0.15
ITS	546 (71)	40	35	87.5	6.4	0.41

[a] Percentage is calculated using the total number of mutations.
[b] Percentage is calculated using the total number of sites.
[c] *p*-Value < 0.05 shows presence of recombination.

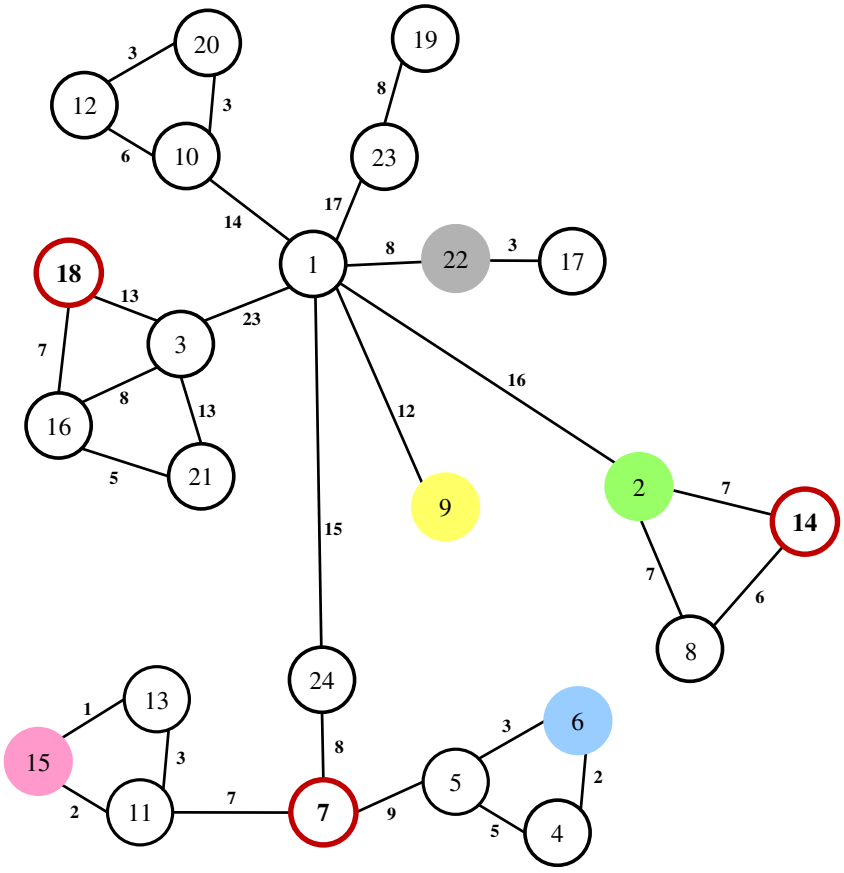

Fig. 8. Haplotype network of *A. infectoria* species–group strains (except *A. photistica* #05) based on maximum parsimony tree of *gpd* sequences. The circles represent the 24 different haplotype groups, which are given in Table 2. The lines between the groups connecting the haplotypes show the number of nucleotides differing. Circles with solid colors (haplotypes 2, 6, 9, 15 and 22) contain more than one strain and circles with red lines (haplotypes 7, 14 and 18) show the position of the recombinant strains.

infectoria species–group depending on the chosen DNA sequence, but was an outlier chemically, having a different metabolite profile. Further research may yield *A. triticina* specific metabolites that can be used to facilitate identification. In food safety, taxa in the *A. infectoria* species–group regularly contaminate cereal grain (Andersen et al., 1996; Pitt and Hocking, 1997; Kosiak et al., 2004; Perelló et al., 2008). The most urgent need is to know what secondary metabolites and other biologically active compounds are produced in the cereals like wheat, barley, and maize. Since current knowledge does not allow connections between metabolite profiles and morpho-species to be made, chemical analyses are needed.

The results presented in this study show that these household genes (ITS, *tef-1α* and *gpd*) do not reflect ecology, secondary metabolism or morphology of the *A. infectoria* species–group and that molecular cladification and phylogeny cannot predict pathogenicity, host specificity or mycotoxin production. Concerning the classification and the systematic placement of the strains and morpho-species in the *A. infectoria* species–group, a polyphasic approach is needed, but there are inconsistencies between the different taxonomic features and we therefore refrain from recommending any taxonomic changes at this point in time.

Acknowledgments

The authors would like to thank EG Simmons for cultures and for suggestions to the manuscript and Jens C. Frisvad and Ulf Thrane for fruitful discussions. This project was a collaboration between CMB, DTU, Denmark and CBS-KNAW, Fungal Biodiversity Centre, The Netherlands and was supported in part by 1) a the SYNTHESYS Project (NL-TAF-1843), http://www.synthesys.info/, which is financed by European Community Research Infrastructure Action under the FP6 "Structuring the European Research Area" Programme", 2) a grant from the Danish Directorate for Food, Fisheries and Agri Business (FFS05-3) and 3) the VILLUM KANN RASMUSSEN foundation.

References

Andersen, B., Hollensted, M., 2008. Metabolite production by different *Ulocladium* species. Int. J. Food Microbiol. 126, 172–179.
Andersen, B., Thrane, U., 1996. Secondary metabolites produced by *Alternaria infectoria* and their use as chemotaxonomic markers. Mycotoxin Res. 12, 54–60.
Andersen, B., Dongo, A., Pryor, B.M., 2008. Secondary metabolite profiling of *Alternaria dauci*, *A. porri*, *A. solani*, and *A. tomatophila*. Mycol. Res. 112, 241–250.
Andersen, B., Hansen, M.E., Smedsgaard, J., 2005. Automated and unbiased image analyses as tools in phenotypic classification of small-spored *Alternaria* spp. Phytopathology 95, 1021–1029.
Andersen, B., Krøger, E., Roberts, R.G., 2002. Chemical and morphological segregation of *Alternaria arborescens*, *A. infectoria* and *A. tenuissima* species–groups. Mycol. Res. 106, 170–182.
Andersen, B., Nielsen, K.F., Thrane, U., Szara, T., Taylor, J.W., Jarvis, B.B., 2003. Molecular and phenotypic descriptions of *Stachybotrys chlorohalonata* sp. nov. and two chemotypes of *Stachybotrys chartarum* found in water-damaged buildings. Mycologia 95, 1227–1238.
Andersen, B., Thrane, U., Svendsen, A., Rasmussen, I.A., 1996. Associated field mycobiota on malt barley. Can. J. Bot. 74, 845–858.
Berbee, M.L., Pirseyedi, M., Hubbard, S., 1999. *Cochliobolus* phylogenetics and the origin of known, highly virulent pathogens, inferred from ITS and glyceraldehyde-3-phosphate dehydrogenase gene sequences. Mycologia 91, 964–977.
Brasch, J., Busch, J.-O., de Hoog, G.S., 2008. Cutaneous phaeohyphomycosis caused by *Alternaria infectoria*. Acta Derm. Venereol. 88, 160–161.
Braun, U., Crous, P.W., Dugan, F., Groenewald, J.Z., de Hoog, G.S., 2003. Phylogeny and taxonomy of *Cladosporium*-like hyphomycetes, including *Davidiella* gen. nov., the teleomorph of *Cladosporium* s. str. Mycol. Prog. 2, 3–18.

Bruen, T., Philippe, H., Bryant, D., 2006. A simple and robust statistical test for detecting the presence of recombination. Genetics 172, 2665–2681.
Butler, E.E., Mann, M.P., 1959. Use of cellophane tape for mounting and photographing phytopathogenic fungi. Phytopathology 49, 231–232.
Carbone, I., Kohn, L.M., 1999. A method for designing primer sets for speciation studies in filametous fungi. Mycologia 91, 553–556.
Christensen, K.B., van Klink, J.W., Weavers, R.T., Larsen, T.O., Andersen, B., Phipps, R.K., 2005. Novel chemotaxonomic markers for the *Alternaria infectoria* species–group. J. Agric. Food Chem. 53, 431–9435.
de Hoog, G.S., Gerrits van den Ende, A.H.G., 1998. Molecular diagnostics of clinical strains of filamentous Basidiomycetes. Mycoses 41, 183–189.
de Hoog, G.S., Horré, R., 2002. Molecular taxonomy of the *Alternaria* and *Ulocladium* species from humans and their identification in routine laboratory. Mycoses 45, 259–276.
Dubois, D., Pihet, M., Le Clec'h, C., Croué, A., Beguin, H., Bouchara, J.-P., Chabasse, D., 2005. Cutaneous phaeohyphomycosis due to *Alternaria infectoria*. Mycopathologia 160, 117–123.
Dugan, F.M., Peever, T.L., 2002. Morphological and cultural differentiation of described species of *Alternaria* from Poaceae. Mycotaxon 83, 229–264.
Dye, C., Johnson, E.M., Gruffydd-Jones, T.J., 2009. *Alternaria* species infection in nine cats. J. Feline Med. Surg. 11, 332–336.
Frisvad, J.C., 1983. A selective and indicative medium for groups of *Penicillium viridicatum* producing different mycotoxins on cereals. J. Appl. Bacteriol. 54, 409–416.
Frisvad, J.C., Samson, R.A., 2004. Polyphasic taxonomy of *Penicillium* subgenus *Penicillium* A guide to identification of food and air-borne terverticillate Penicillia and their mycotoxins. Stud. Mycol. 49, 1–173.
Frisvad, J.C., Thrane, U., 1987. Standardized high-performance liquid chromatography of 182 mycotoxins and other fungal metabolites based on alkylphenone retention indices and UV–VIS spectra (diode array detection). J. Chromatogr. 404, 195–214.
Hansen, M.E., 2003. Indexing and analysis of fungal phenotypes using morphology and spectrometry. Ph.D. Thesis. IMM, DTU, Denmark. ISSN 0909-3192.
Haubold, B., Hudson, R.R., 2000. LIAN 3.0: detecting linkage disequilibrium in multilocus data. Bioinformatics 16, 847–849.
Huson, D.H., Bryant, D., 2006. Application of phylogenetic networks in evolutionary studies. Mol. Biol. Evol. 23, 254–267.
Kosiak, B., Torp, M., Skjerve, E., Andersen, B., 2004. *Alternaria* and *Fusarium* in Norwegian grains of reduced quality – a matched pair sample study. Int. J. Food Microbiol. 93, 51–62.
Kwasna, H., Kosiak, B., 2003. *Lewia avenicola* sp nov and its *Alternaria* anamorph from oat grain, with a key to the species of *Lewia*. Mycol. Res. 107, 371–376.
Laatsch, H., 2008. AntiBase 2008. The Natural Compound Identifier. Wiley-VCH GmbH & Co., Weinheim, Germany.
Nielsen, K.F., Smedsgaard, J., 2003. Fungal metabolite screening: database of 474 mycotoxins and fungal metabolites for dereplication by standardised liquid chromatography-UV–mass spectrometry methodology. J. Chromatogr. A 1002, 111–136.
Nielsen, K.F., Gräfenhan, T., Zafari, D., Thrane, U., 2005. Trichothecene production by *Trichoderma brevicompactum*. J. Agric. Food Chem. 53, 8190–8196.
O'Donnell, K., Ward, T.J., Geiser, D.M., Kistler, H.C., Aoki, T., 2004. Genealogical concordance between the mating type locus and seven other nuclear genes supports formal recognition of nine phylogenetically distinct species within the *Fusarium graminearum* clade. Fungal Genet. Biol. 41, 600–623.
Pedras, M.S.C., Chumala, P.B., 2005. Phomapyrones from blackleg causing phytopathogenic fungi: isolation, structure determination, biosyntheses and biological activity. Photochemistry 66, 81–87.
Perelló, A.E., Sisterna, M.N., 2006. Leaf blight of wheat caused by *Alternaria triticina* in Argentina. Plant Pathol. 55, 303.
Perelló, A.E., Moreno, M., Sisterna, M.N., 2008. *Alternaria infectoria* species–group associated with black point of wheat in Argentina. Plant Pathol. 57, 379.
Pitt, J.I., Hocking, A.D., 1997. Fungi and Food Spoilage. Blackie Academic and Professional, London, UK.
Prasada, R., Prabhu, A.S., 1962. Leaf blight of wheat caused by a new species of *Alternaria*. Indian Phytopathology 15, 292–293.
Pryor, B.M., Bigelow, D.M., 2003. Molecular characterization of *Embellisia* and *Nimbya* and their relationship to *Alternaria*, *Ulocladium* and *Stemphylium*. Mycologia 95, 1141–1154.
Rosendahl, S., 2008. Communities, populations and individuals of arbuscular mycorrhizal fungi. New Phytologist 178, 253–266.
Rozas, J., Rozas, R., 1995. DnaSP, DNA sequence polymorphism: an interactive program for estimating Population Genetics parameters from DNA sequence data. Comput. Applications Biosci. 11, 621–625.
Salemi, M., Gray, R.R., Goodenow, M.M., 2008. An exploratory algorithm to identify intra-host recombinant viral sequences. Mol. Phylogenet. Evol. 49, 618–628.
Samson, R.A., Noonim, P., Meijer, M., Houbraken, J., Frisvad, J.C., Varga, J., 2007. Diagnostic tools to identify black *Aspergilli*. Stud. Mycol. 59, 129–145.
Simmons, E.G., 1986. *Alternaria* themes and variations (22–26). Mycotaxon 25, 287–308.
Simmons, E.G., 2007. *Alternaria*. An Identification Manual. CBS Fungal Biodiversity Centre, Utrecht, The Netherlands.
Simmons, E.G., Roberts, R.G., 1993. *Alternaria* themes and variations (73). Mycotaxon 48, 109–140.
Stamatakis, A., Hoover, P., Rougemont, J., 2008. A rapid bootstrap algorithm for the RAxML web-servers. Syst. Biol. 75, 758–771.
Taylor, J.W., Jacobson, D.J., Kroken, S., Kasuga, T., Geiser, D.M., Hibbett, D.S., Fisher, M.C., 2000. Phylogenetic species recognition and species concept in fungi. Fungal Genet. Biol. 31, 21–32.
Wägele, J.W., Mayer, C., 2007. Visualizing differences in phylogenetic information content of alignments and distinction of three classes of long-branch effects. BMC Evol. Biol. 7, 147–170.
White, T.J., Bruns, T., Lee, S., Taylor, J., 1990. Amplification and direct sequencing of fungal ribosomal RNA genes for phylogenetics. In: Innis, M.A., Gelfand, D.H., Sninsky, J.J., White, T.J. (Eds.), PCR Protocols: A Guide to Methods and Applications. Academic Press, San Diego, pp. 315–322.